Adoption of a Performance Evaluation Technique for the Development of a Framework for the Climatic Responsive Urban Design (CRUD)

Salma Sherbaz & Humera Mughal

(CGP #01-135)

RASTA CONFERENCE

Monday 28th & Tuesday 29th March 2022

PC Bhurban, Murree

This document is unedited author's version submitted to RASTA.

RESEARCH FOR SOCIAL TRANSFORMATION & ADVANCEMENT

Pakistan Institute of Development Economics

Islamabad

TABLE OF CONTENTS

LIST OF TABLES

LIST OF FIGURES

INTRODUCTION

1.1 Urbanization

The mass influx/migration of human population from ruler area and resulting changes in urban settings is known as urbanization. The concept of urbanization goes a long way back in human history, just to fulfill the water and food requirements of large populations [1]. However, the industrial revolution in the late eighteenth century promoted rapid growth in the urban population, first in Europe and later in other parts of the world. A significant increase in the percentage of the world population living in urban areas has been observed over the past few decades. In 1950, around 30% of the worldwide population lived in urban areas. By 2007, for the first time in human history, more than 50% of the world's population was urban. As per the United Nation's updated estimates for the year 2018, 55% of the world's population was living in urban areas and is expected to increase to 68% by 2050[2].

In the case of Pakistan, a similar steady trend in the growth rate of the urban population has been observed. In Pakistan, the annual percentage growth in the urban population was around 2.7% in 2019 [3]. So, to accumulate the increasing number of incoming habitats, our cities need to further develop themselves and improve the urban environment.

1.2 Challenges of Urbanization

Although urbanization is mostly considered as an indicator of economic, social, and political progress of a society, it can also lead to several challenges including urban sprawl, environmental and health issues, increasing crime and human insecurity related problems, poor urban governance, weak financial capacity of cities and higher living cost, etc. [2]. Urban areas have significant energy consumption and CO_2 emissions footprint [4]. Although the urban areas only cover 0.4–0.9% of the global land surfaces [5], their contribution to the global CO_2 emissions is more than 70% [6,7]. The negative impacts of rapid urbanization on the environment are profound and reach far beyond urban settlements themselves [8].

The global environment has changed for the worse and our country, Pakistan, is no exception. A slight glance at the annual mean temperature, Sealevel, and rainfall patterns is ample to portend the looming crisis. During the past half-century, the country's mean temperature has gone up more than half a degree Celsius, its coast's sea level increases more than ten centimeters, and its rainfall and heat-wave patterns altered to levels of disbelief. The prediction for the next century, estimating an up to a six-degree Celsius increase in the average annual temperature and an up to sixty-centimeter rise in the mean sea level, is horrific and far beyond the accounts of human history[9].

Urban Heat Island Phenomenon

The urban heat island (UHI) effect is a common environmental problem faced by the urban areas in which their air temperature is significantly higher than surrounding suburban areas. Compact development in urban areas is the main reason for UHI as the high concentration of building structures not only limits airflow but also emits heat stored from solar energy. The previous

research studies suggest that due to UHI, the day and nighttime temperatures in urban areas are 1–7°F and 2–5°F higher than the rural areas respectively [10].

Causes of UHI

Several factors cause heat islands:

Low Plantation and Water Bodies: Plants trigger the process of transpiration, providing shade and evaporating surface water into the air, hence cooling the surrounding environment. On the other hand, Hardscapes, paved areas, and buildings provide no moisture and less shade, and therefore, contribute more towards temperature gain, resulting in higher temperature.

Urban Building Material Properties: Materials like stone, marble, and concrete used in construction sectors such as paving, and roofing absorb and later emit more heat as compared to the green natural surfaces like plants and vegetation.

Urban Street Morphology: The street orientation, length height to width (H/W) ratios, and sky view factor have a significant effect on wind and heat distribution inside an urban street canyon. Surfaces and structures in densely built urban areas are obstructed by neighboring buildings hence providing no path for heat circulation and becoming large thermal masses. So, the knowledge of flow characteristics in street canyons is an important consideration for Climate-responsive urban design.

Human-generated activities/sources of heat: Industrial facilities, vehicles, buildings, air-conditioning units, and all emit heat into the urban environment and contribute to heat island effects

Weather and Geography: Calm and clear weather maximizes the amount of solar energy that is reached and absorbed by the urban surfaces and hence increases the urban heat island. On the other hand, cloud cover and strong windy weather conditions suppress the formation of the heat island.

Effects of UHI

UHI affects us in more ways than we normally realize. A localized increase in temperature for any urban area in general and one in Pakistan creates a host of issues. Being an inherently energy-starved country, coping with the higher energy demands in summer has always been impossible and whatever make-shift remedy the policymakers opted for has bred more problems than before the intervention had been undertaken. For instance, the rise in the urban temperature in summer can easily reach twenty to twenty-five Celsius. Such an exorbitant rise in temperature causes an exponential increase in air-conditioning and hence, an up to 10 percent surge in energy demand.

In the heated frenzy, the power plants operating on fossil fuels are turned on, completely disregarding their contribution to the emission of greenhouse gases and air pollutants that feed the fire people feel in the urban areas. In desperation, even more, refrigeration is deployed, perpetuating the vicious cycle of fueling the fire. The rise of temperature does not only prompt higher energy consumption but can go as far as triggering thunderstorms and altering the precipitation trend.

The UHI's ramification on the health of the masses is also incredibly significant. From mere uneasiness to the loss of consciousness, repeatedly attributed to the heat waves, are exacerbated by the UHI.

1.3 Land use Planning and Urban Climate

The economic value once dominated the economy-ecology balance in the urban expansion process around the world. But now rapid and irregular urban development has become a global concern and the current continuation in the severity of this problem seems inevitable shortly.

Land use planning in terms of preparation, arrangement, and allocation of land use is a vital part of sustainable land management (SLM) and can have a positive or negative effect on the state of the environment[11]. Moreover, urban land use and the surface cover is considered as an indicator of urban environmental and ecological landscape characteristics. The urban form has a significant effect on the thermal environment, overall air quality, and energy demand[12–14].

1.4 Urban Climate Modeling and Assessment

The research studies on urban climate modeling and assessment are usually performed on four different spatial scales (in the horizontal direction) i.e. mesoscale, microscale, building scale, and indoor. Mesoscale modeling is the study of phenomena in larger areas (<200 km). With the recent advancements of numerical approaches and computational resources, an increase in the number of urban mesoscale modeling studies has been observed in the past few decades [15]. These studies are mostly focused on calculation and mitigating of the urban heat island (UHI) effect, air pollution assessments, weather forecasts improvements, etc. [16–20]. The micro-scale extends from less than one meter to hundreds of meters including individual buildings, roads, trees, courtyards, lawns, etc. Building scale urban studies consider the small areas (<100m) having individual buildings or few blocks. The indoor climate-related study only considers the interior of a building (<10m) and is mostly aimed at heating, ventilation, and air conditioning (HVAC) system design and building services engineering to create optimal indoor environments.

1.5 Urban Microclimate

Urban Microclimate Descriptors and Controlling Factors

The urban microclimate is the result of several dynamic and complex processes that interact at multiple spatial and temporal scales. The varied factors that can affect the microclimate in an urban setup can be divided into the following three main categories[21]:

a) *Natural Factor:* wind direction, speed, precipitation, humidity, solar radiation, albedo, greenery, natural water bodies, soil type, and terrain conditions
b) *Built Environment*: Building characteristics (material, height, shape, texture, color), street canyon characteristics (canyon aspect ratio (AR), sky-view factor (SVF), length and orientation), Urban greenery (street trees and urban parks), man-made water bodies, population density, road traffic density, and anticipated traffic volume, built-up area vs open space ratio, location, and type of industry
c) *Indirect Factors*: Air pollution, ongoing construction/development activities

The different urban microclimate descriptors used in the literature are broadly divided into six categories i.e. (as shown in Figure 1.1)[22]:

- Temperature related descriptors
- Thermal comfort-related descriptors
- Heat transfer related descriptors
- Flow/ventilation related descriptors
- Humidity/mass transfer related descriptors
- Dimensionless numbers/indices related descriptors
- Other quantitative parameters

Figure 1: Urban microclimate descriptors

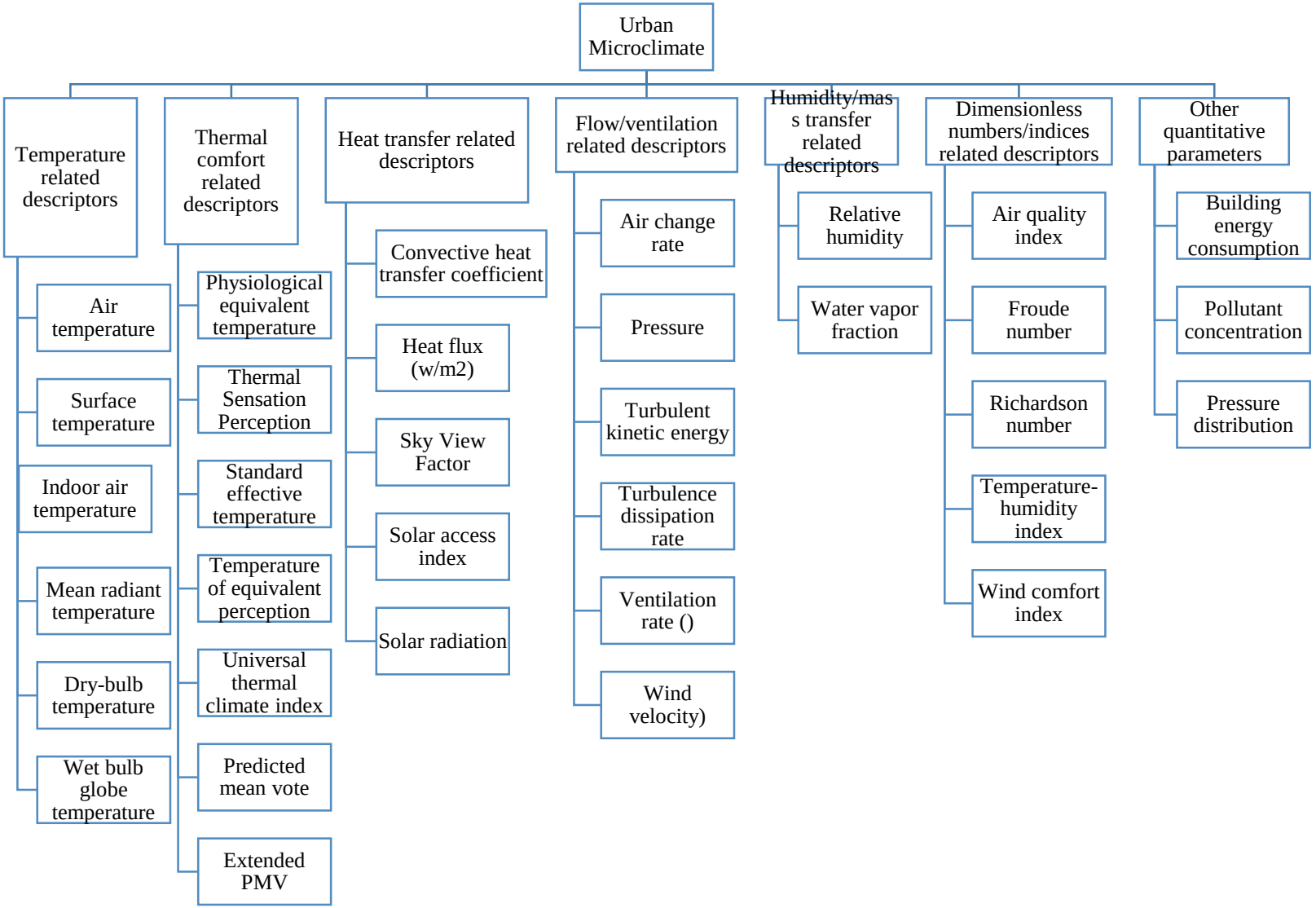

Urban Microclimate Assessment

Since the pioneering works of Luke. Howard, numerous studies have been performed in the area of urban microclimate [23]. These studies not only improve the general understanding of the energy balance in the built environment but also explain/elaborate interactions between urban structural forms and its microclimate. This knowledge is extremely helpful for urban designers and architects in creating a climate-responsive urban design.

Urban microclimate can be studied using several different approaches which can be divided into two main groups[24,25]. There are several advantages as well as challenges associated with each of these approaches.

a) *Observational approaches: Field measurements, thermal remote sensing, and small-scale modeling*

b) *Simulation approaches.*

The field measurements, thermal remote sensing, and small-scale modeling of urban microclimate are the main techniques included in the first category [24,25]. Collecting the data from fixed weather stations is a traditional observational approach. However, this data is not considered a true representation of the city's microclimate, due to several changes in impervious surfaces, vegetation cover, and waste heat from buildings and vehicles throughout the city [26]. Similarly, the installation of the different measurement devices throughout a city is generally expensive and time-consuming. With the recent advancement of sensor technology, it is often used independently or combined with in situ measurements to collect data on land cover and ground surface temperatures. The temporal and spatial resolution and cost associated with remote sensing techniques remain significant limitations [26]. Similarly, with the availability of powerful computers and new methods for modeling complex systems, an increasing trend in the application of numerical simulation approaches in urban microclimate studies has been observed. However, complex urban details, the high computational cost of such simulations are a few challenges associated with these approaches.

1.6 Research Structure

The goal of this research is to guide the designer for the early-stage climate responsive urban design

Hypothesis: It is considered that the different urban design elements i.e. street canyon geometry (Canyon length, width, height, orientation, and SVF) and greenery have an impact on the urban microclimate which affects the energy load and thermal comfort in the built environment.

Overall Objective: The goal of this research may be achieved by the development of a framework named CRUD (climate-responsive urban design) for the optimization of urban street canyon geometry (Canyon length, width, height, orientation, and SVF) in an urban district. Sub objectives of this research are:

a) Study of already developed urban design of the various cities of Pakistan.

b) Performance evaluation of the design by evaluating the effect of different the different urban design elements i.e. street canyon geometry (Canyon length, width, height, orientation, and SVF) and greenery on the urban microclimate.
c) Development of a framework to develop the optimum design layouts based on a performance evaluation technique.
d) Application of the framework for the development of a small sector in Islamabad, Pakistan.

LITERATURE REVIEW

The urban microclimate is affected by geographical, seasonal, and meteorological (e.g., wind speed and cloud cover) variables. In addition, several location-specific factors including site geometry and its spatial location (i.e. proximity to parks or water bodies) also control its microclimate.

The urban climate is an effective issue on the local and global climates which is influenced by several factors such as urban morphology and density, the properties of urban surfaces, and vegetation cover. The inappropriate using of these factors could change the microclimate of urban areas.

2.1 Canyon Geometry Descriptors and Microclimate

Urban canyons (UCs) are considered as basic urban units of a typical urban setting and the central spatial core of its climatic conditions. In literature, the urban street canyon is mostly classified based on its geometrical specifications i.e. canyon length, sky view factor, aspect ratio (H/W ratio), and orientation[27][28]. Several researchers have extensively studied the relationship between these canyon geometry descriptors and urban microclimate. The details of recent studies and important conclusions are given in table 2.1

Table 1: Summary of previous studies

Location	Climate	Urban Design Variables	Factors monitored	Important Conclusions	Ref
Campinas, Brazil	Hot and humid (subtropical)	Street Orientation (15-degree interval), Height to width ratio	Thermal comfort, physiologically equivalent temperature (PET)	1. A northeast-southwest orientation had a significant reduction PET during daytime. 2. A H/W ratio up to 2 increased thermal comfort by increasing shade 3. For H/W less than 0.5, forestry management and green areas were recommended for the augmentation of shade.	[29]
Bangkok, Thailand	Tropical	Street Orientation (4), Height to width ratio, Canyon height	Urban ventilation (Wind velocities)	1. The wind velocity is high in the shallow and long deep canyons.	[30]
Ghardaia-Algeria	Hot and dry	Street Orientation (E–W, N–S, NE–SW, and NW–SE), Height to width ratio	Physiologically equivalent temperature (PET), Mean radiant temperature	1. The thermal environment for wide streets (H/W=0.5) is highly stressful and almost independent of the orientation. 2. For a H/W≥2 N–S, NE–SW or NW–SE orientation streets provides a much better thermal environment .	[27]

Ghardaia-Algeria	Hot and dry	Street Orientation (E-W, N-S, NE-SW, NW-SE), Height to width ratio using galleries, canyon asymmetry	Physiologically equivalent temperature (PET), Air temperature	1. Galleries, overhanging facades, vegetation, and street canyon asymmetry have a strong effect on the thermal sensation as compared to air temperature 2. A large value of sky view factor is linked with high thermal stresses irrespective of a particular orientation. 3. The orientation is important for canyons with a smaller sky view.	31
Tunis, Tunisia	Subtropical Mediterranean (Mediterranean subtropical climate)	Street orientation, Height to street width ratio, Sky view factor	Wind speed, air temperature, mean radiant temperature, and relative humidity	1. In the summer season deepest streets canyons offer acceptable conditions in terms of thermal comfort 2. For all H/W ratios , NS-oriented canyons were found as most comfortable whereas E-W-oriented-oriented canyons experienced the worst degree of comfort.	32
Stuttgart, Germany		Street Orientation (One street at 0–165-degree rotation), Height to width ratio	Physiologically Equivalent Temperature (PET), mean radiant temperature, air temperature, vapor pressure, wind speed	1. Around 10^{o}C and 25^{o}C reduction in PET values due to trees as compared to green and sealed areas respectively. 2. northwest-southeast oriented street canyon having an aspect ratio of at least 1.5 possess low thermal stress.	33
Dhaka, Bangladesh	tropical warm-humid	Street Orientation (E–W, N–S, E–W, and N–S)	3. Air temperature, mean radiant temperature, relative humidity, and wind velocity	For two urban areas with different urban geometry features 1. A 3.3°C and 6.2°C difference in average and maximum air temperature 2. 2.3 °C and10.0°C difference in average and maximum T_{mrt}	34
Netherlands	hot arid and humid	Different urban forms (singular, linear and courtyard) Street Orientation (E–W, N–S)	Air temperature, mean radiant temperature, wind speed, relative humidity, Physiological Equivalent Temperature	1. Courtyards provided the most comfortable microclimate during a summer day. 2. N-S oriented street canyons had a cooler microclimate	35

Hamadan City in Iran	the cold and mountainous climate	Street Orientation (E–W, N–S, NE–SW, and NW–SE), sky view factor	Air temperature, mean radiant temperature, wind speed, relative humidity, Physiological Equivalent Temperature	1. The north-south-oriented streets are more desirable for the Winter season with average 4.5-8 °C high PET values. 2. For the Summer season, northeast-southwest and northwest-southeast oriented streets provide better thermal comfortable by providing lowest PET (about 2 °C cooler than other orientations)	[36]
Riyadh City, Saudi Arabia	hot-arid climate	Street Orientation (EW, NS, NE-SW, and NW-SE), Height to width ratio, sky view factor	Outdoor Thermal Comfort, Air temperature, mean radiant temperature, Wind velocity, Energy consumption	1. NE-SW oriented canyons had the lowest PET values as compared to all other orientations	[37]
Southern, China	Hot-Humid	Length-width ratio, canyon types, canyon axis orientation	Wind velocity, Air temperature, mean radiant temperature, PET	1. Greenery and arcades can improve pedestrian-level thermal comfort in E-W orientation streets. 2. Boulevards having an aspect ratio greater than 0.67, dense greenery is recommended. 3. Arcade streets are a better option for neighborhoods with longer E-W oriented streets and shorter N-S orientation	[38]

METHODOLOGY

3.1 Study Area

The present study was carried out in Islamabad (planned) and Rawalpindi (semi-planned) located at 33.662883° Lat, 73.086373°Lon. Islamabad is the Federal Capital of Pakistan and with a current area of 906 km^2, it is becoming a fast-growing city of Pakistan. According to United Nations Habitat 2020 report, the land consumption rate in Islamabad was 4.77 percent during the years 2000 – 2015, much higher as compared to other cities of Pakistan. A similar trend has been observed in the rate of population growth in Islamabad[39]. Rawalpindi is a city in the Potwar Plateau, near Islamabad, and the two are jointly known as the "twin cities" on account of their strong social and economic linkage. With an area of 259 km^2, the estimated population of Rawalpindi is about 2.2 million.

Table 2: Land Consumption and Population Growth Rates between 2000-2015[39]

City Name	Land Consumption Rate 2000 - 2015 (%)	Population Growth Rate 2000 - 2015 (%)
Islamabad	4.77	2.56
Quetta	4.37	0.67
Karachi	1.72	2.23
Peshawar	1.91	1.78
Lahore	3.25	1.87

Urban fabric and weather

Islamabad was planned by Constantinos A. Doxiadis and Doxiadis Associates in the late 1950s on a grid-iron pattern. The formal grid of 2km x 2km divides the whole city roughly into 84 sectors. separated by the network of wide principal roads (600 ft.). On the other hand, high population growth has resulted in uncontrolled urban sprawl in the case of Rawalpindi, resulting in a complex urban fabric. Unlike Rawalpindi, Islamabad has a proliferating green cover. As far as the surface texture is concerned, the streets in both cities are covered by asphalt and concrete.

The Street network orientation of both cities is visualized using OSMnx tool. OSMnx is a Python package that uses geospatial data from OpenStreetMap to analyze and visualize the street grid of any city of interest[40]. In the polar histograms (Figure 4.1(a) and (c)), the direction of each bar orientation of the streets and its length represent the relative frequency of streets with those orientations. It can be observed that in the case of Islamabad, Streets are well-structured, in ENE-WSW (making 34^0 -angle with east) or NNW-SSE (making 124^0 with east) direction, forming the gridiron pattern (shown in Figure 4.1 (b)). As far as the texture is concerned, the streets are covered by asphalt and concrete and mostly shaded by young trees in the middle of streets (near street-view). On the other hand, Rawalpindi features a grid in small neighborhoods, but mostly its streets are distributed in every direction, resulting in an organic urban fabric.

Figure 2: Street networks and corresponding polar histograms for (a) Islamabad and (b)

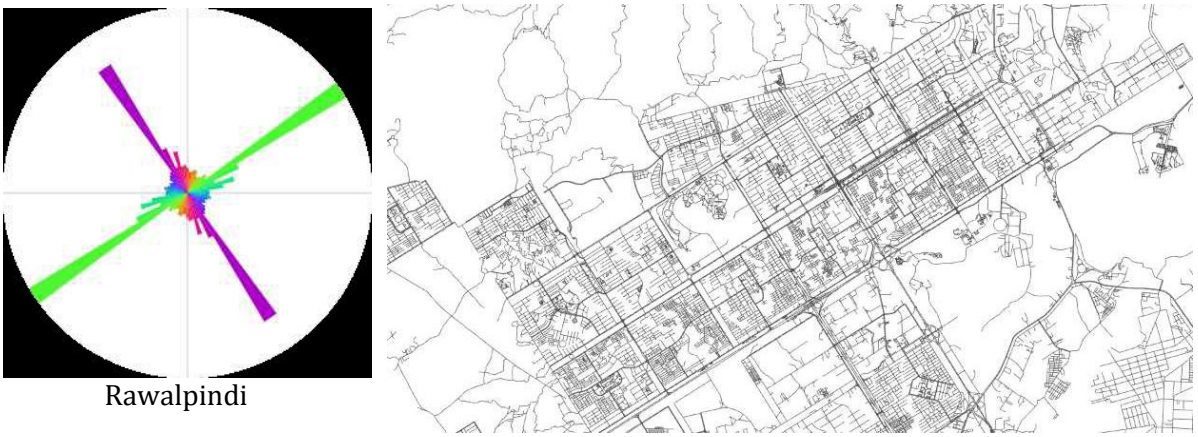

Rawalpindi

As per Koppen climate classification, twin cities have monsoon-influenced humid subtropical climates (Cwa) i.e. it hasmild dry winters and hot humid summers [41].

Figure 3: Islamabad average climate

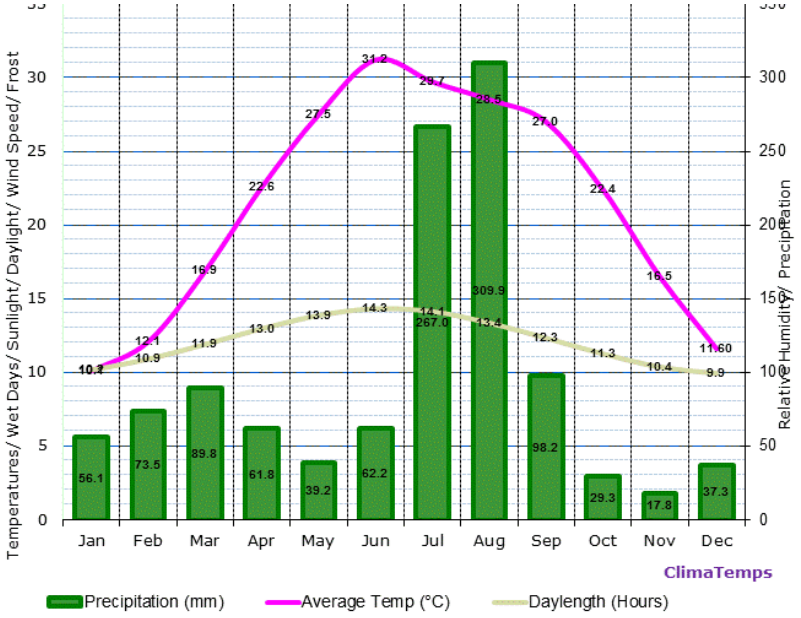

3.2 Land Cover and Land Use (LULC) Maps of Twin Cities

Land Use and Land Cover (LULC) generally refers to the categorization or classification of human activities and natural elements on a certain landscape. The LULC can have a significant impact on the local and regional climate dynamics [25]. These classification maps are very important for a spatial understanding of local climate and the design of an urban form based on climatic consideration. Several LULC classification schemes have been developed in the past i.e. Urban Zones of Energy partitioning (UZE) [26, 27], Urban Climatic Map (UCMap) system[28], Urban Climate Zone (UCZ) scheme[29] and Local Climate Zone (LCZ) scheme[30]. All of these schemes have used topographic, surface geometry, land use/land cover (LU/LC) patterns, and climatic spatial information as urban indicators.

In literature, several researchers have employed the concept of LCZ to quantify the correlation between urban morphology and UHI. LCZ classification scheme consists of 17 classes/climate zones where each LCZ class is a depiction of "regions of uniform surface cover, structure, material, and human activity" (as shown in Figure 3.3) and has a uniform temperature. A typical LCZ class can extend from a few hundred meters to several kilometers on a horizontal scale[30].

Figure 4: LCZ Concept Visualization

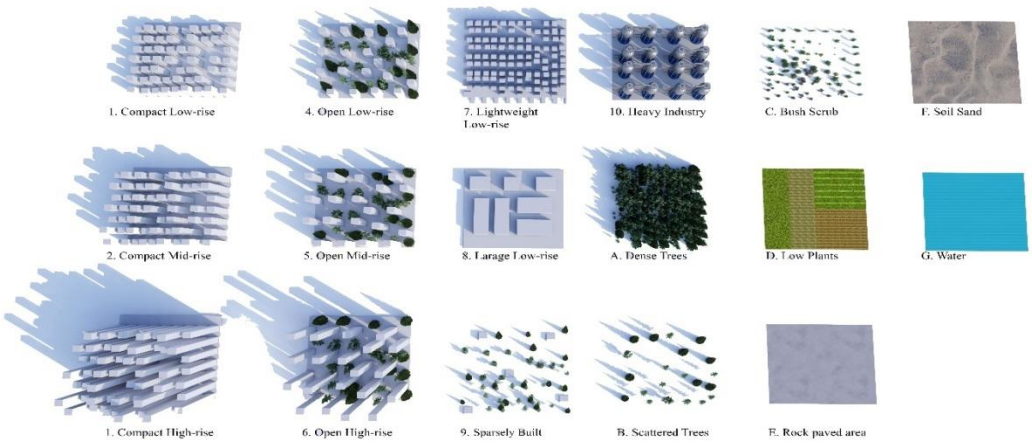

So following the Local Climate Zone (LCZ) scheme, both cities, Islamabad and Rawalpindi, have been classified based on climate-relevant surface properties. The training data of LCZ classification was generated using high-resolution satellite imagery in Google Earth Pro. The number of training samples created for each LCZ class is presented in Figure 3.4. The World Urban Database and Access Portal Tool (WUDAPT) web-based application is used for the generation of complete LCZ maps based on our training data. WUDAPT classification tool uses Landsat images and random forest (RF) classifier present in the System for Automated Geoscientific Analyses (SAGA) software.

Figure 5: Training area samples in twin cities defined using Google Earth imagery

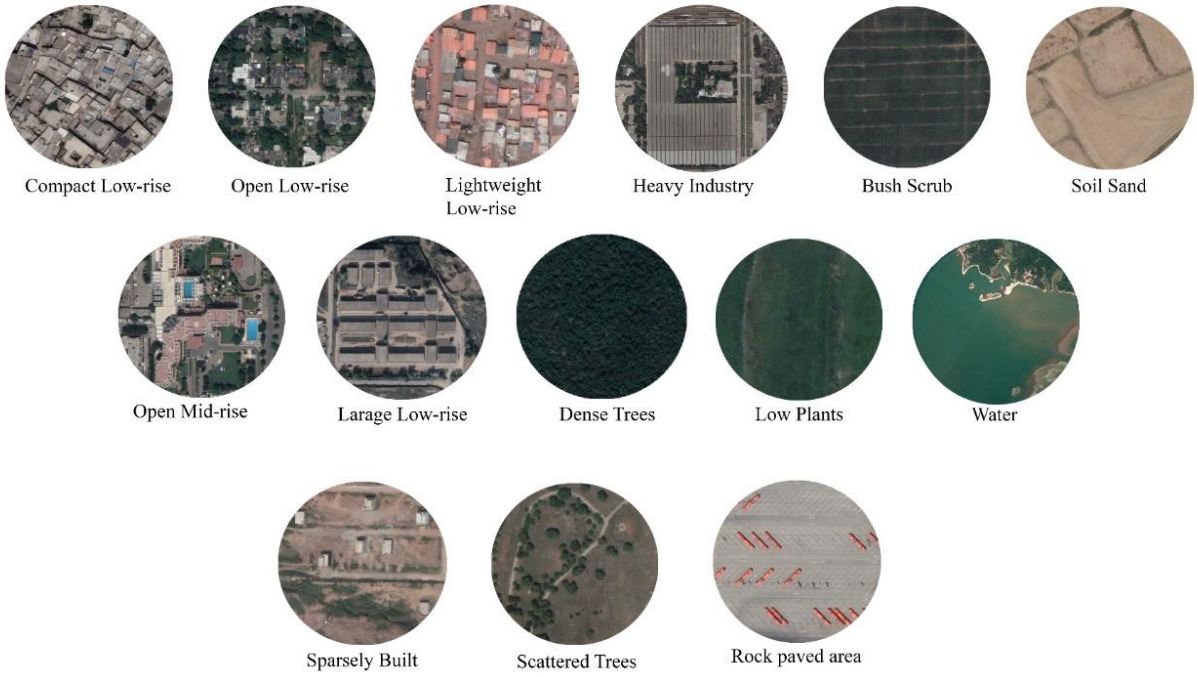

The accuracy of the generated LCZ maps of Islamabad and Rawalpindi (shown as Figure 3.5) is assessed in termsof producer's accuracy (PA), user's accuracy (UA), and overall accuracy (OA), the overall accuracy of the urban LCZ classes only (OAu), the overall accuracy of the built vs. natural LCZ classes only(OAbu) and a weighted accuracy (OAw). The boxplot figure with accuracies is shown in Figure 3.6. The overall accuracy is 82 %.

Figure 6: Number of training areas per LCZ class

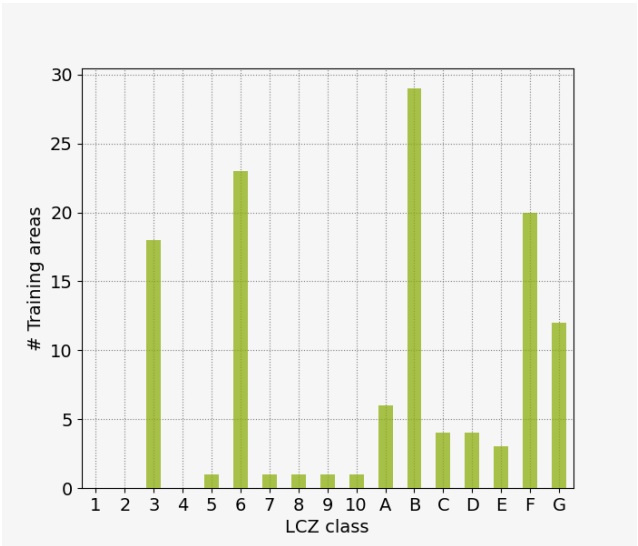

Figure 7: LCZ classification map of (a) Islamabad; (b) Rawalpindi

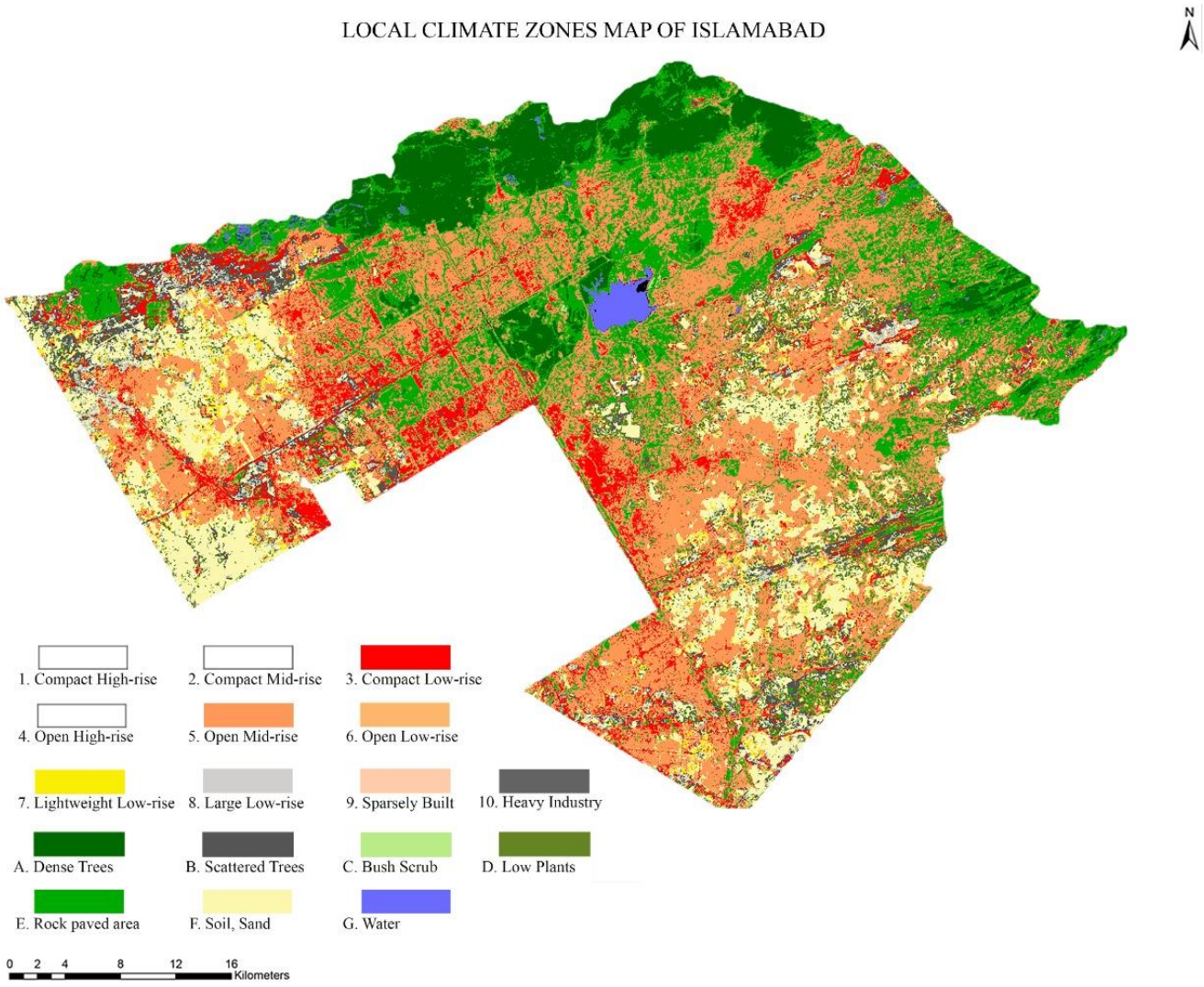

(a)

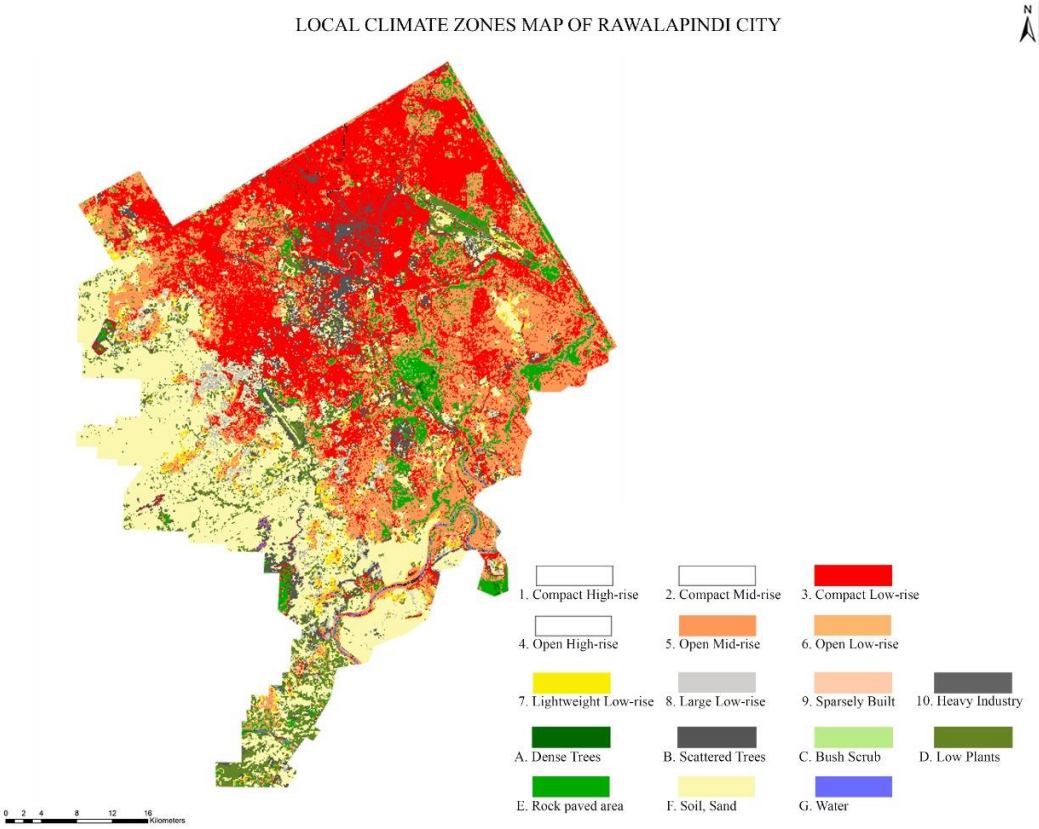

(b)

Figure 8: Boxplot figure with accuracies

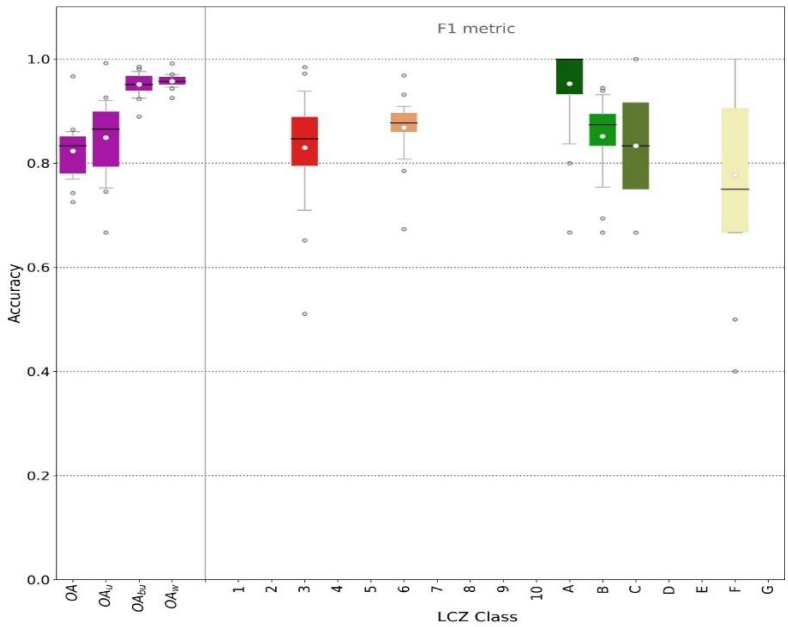

3.3 Data Collection

The accurate measurement of the different urban design elements i.e. street canyon geometry (canyon length, width, height, orientation, and SVF) and greenery is required to assess the impact of these variables on urban microclimate. In the case of Islamabad, the data regarding the lengths, widths, height, and orientation of the different street canyons is acquired from the capital development authority (CDA). These measurements were further confirmed in the field survey.

In the case of Rawalpindi, lengths, widths, height, and orientation of the different street canyons are calculated during the field survey. For both Rawalpindi and Islamabad, the greenery type and distribution within different street canyons are recorded during field measurements.

To calculate the sky-view factor of the different street canyons in twin cities, fisheye images were captured during the field survey. These images were then segmented into the sky and non-sky pixels (shown in Figure 3.8).

Figure 9: A fisheye image of a street canyon in (a) Islamabad; (b) Rawalpindi

(a)

(b)

3.4 Remote-Sensing (Rs) Based Assessment of Urban Microclimate

Land surface temperature (LST) is an important microclimate parameter as its temporal and spatial variations within a city indicate the city's thermal environment and behavior[42]. The retrieval of the LST from remotely sensed thermal infrared (TIR) data has attracted a great deal of attention in recent years[43]. Since then, different methods having different mathematical

formulas and input parameters have been developed to retrieve the LST from space-based remote sensing images[44,45]. However, all these methods include the estimation of spectral radiation and brightness temperature[46].

In the present study, the freely available satellite (LANDSAT 8) images have been used for the retrieval of LST. The required data is downloaded from the United States Geological Survey (USGS) (http://landsat.usgs.gov) website. The Landsat-8 imagery of Twin cities used in the present study was acquired at 05:42 UTC (about 10:42am local standard time) on July 02, 2021. The TIR band 10 is used for estimation of brightness temperature whereas visible red (R) and near-infrared (NIR) bands 4 and 5 are used for calculating the Normalized Difference Vegetation Index (NDVI). The steps involved in the calculation of LST are given below:

***Step 1*:** Top of Atmospheric Spectral Radiance

The top of atmospheric (TOA) spectral radiance (L_λ) was calculated using the following relationship:

$$L\lambda = M_L * Q_{cal} + A_L - O_i$$

where $M_L$and A_L are the band-specific multiplicative and additive rescaling factors, Qcal is the Band 10 image, and Oi is the correction for Band 10[46].

Step 2: Conversion of Radiance to At-Sensor Temperature

The band-specific thermal conversion constants $K1$ and $K2$ were employed to calculate brightness temperature (BT) using the following relationship:

$$BT = \frac{K_2}{ln\,[(K_1/L\lambda) + 1]} - 273.15$$

The absolute zero (approx.−273.15◦) is added to get the result in degree Celsius[47].

Step 3: NDVI Calculation

The visible red (R) and near-infrared (NIR)bandsofLandsat8 were used for calculating the Normal Difference Vegetation Index (NDVI).

$$NDVI = \frac{NIR\ (band\ 5) - R\ (band\ 4)}{NIR\ (band\ 5) + R\ (band\ 4)}$$

Where Rrepresents the red band (Band 4).

Step 4: Proportional vegetation (PV) Calculation

NDVI values obtained in step 3 are used for the calculation of proportional vegetation (Pv) employing the following relationship[48]:

$$PV = \left(\frac{NDVI - NDVI_{min}}{NDVI_{max} - NDVI_{min}}\right)^2.$$

The NDVI index is close to one in the area having dense vegetation and to −1 in case of poor vegetation.[49]

Step 5: Calculation of land surface emissivity (LSE)

The below equation is used to determine the LSE (ε):

$$\varepsilon = 0.004 * PV + 0.986$$

Step 6: LST calculations

For LST calculations, the previously calculated results of BT and LSE are used as per the following equation:

$$LTS = \frac{BT}{1+\left\{\left(\frac{\lambda BT}{\rho}\right) ln\varepsilon_{\lambda}\right\}}$$

Where LST is the land surface temperature in Celsius (°C), λ is the average wavelength of band 10, $\varepsilon_{\lambda}$is the land surface emissivity calculated in step 5and ρ = 14380.

3.5 Comutational Fluid Dynamics Based Assessment of Urnab Microclimate

The use of computational fluid dynamics (CFD) simulation for urban microclimate assessment makes it possible to consider the detailed modeling of every building and the parameterization of other obstacles within a selected urban area. With the recent advancements in numerical approaches, computational resources, and the establishment of CFD best practice guidelines on the relevant topics[50–52], the use of CFD for urban microclimate assessment studies is becoming increasingly popular[22]. The different Open source and commercial CFD software are being used for the urban microclimate simulation including CFD series, ENVI-Met, OpenFOAM, AnsysFluent, Phoenics etc[53]. Any CFD software is based on the three basic principles of physics i.e., mass, momentum, and energy conservation expressed mathematically as:

$$\frac{\partial \rho}{\partial t} + \nabla.(\rho u) = 0$$

$$\frac{\partial \rho u}{\partial t} + \nabla.(\rho u u) = -\nabla p + \nabla.\tau + F$$

$$\frac{\partial}{\partial t}\left[\rho\left(e + \frac{1}{2}u^2\right)\right] + \nabla.\left[\rho u\left(e + \frac{1}{2}u^2\right)\right] = \nabla.(k\nabla \mathrm{T}) + \nabla.(-pu + \tau.u) + u.\mathrm{F} + Q$$

The solution to the above system of coupled nonlinear partial differential equations gives the temporal and spatial variation of velocity (v), pressure(p), and temperature (T) of the fluid in the entire flow domain.

In the present study, urban flow simulations have been performed using Envi-met software. The Envi-met is a frequently used software for environmental analysis and urban planning. Ever since its first release in 1998, until 2017, more than 1900 registered users worldwide used Envi-met in microclimate-related research applications[54]. The main reason for its wide popularity is since it allows the possibility of considering the complex urban geometry, position of the sun, various surface types, building materials, and vegetation.

Every CFD simulation problem has the same workflow which can be divided into three basic steps i.e., pre-processing, processing, and post-processing. The preprocessing includes model development and mesh generation, specification of flow properties, and initial and boundary conditions. Processing implies specifying the solver parameters and discretization schemes, etc. Post-processing is the last step in the CFD workflow, and it involves the visualization and interpretation of simulation results. The details on the preprocessing performed in the present study are given in the following paragraphs:

Figure 10: LST (0C) map of (a) Islamabad; (b) Rawalpindi

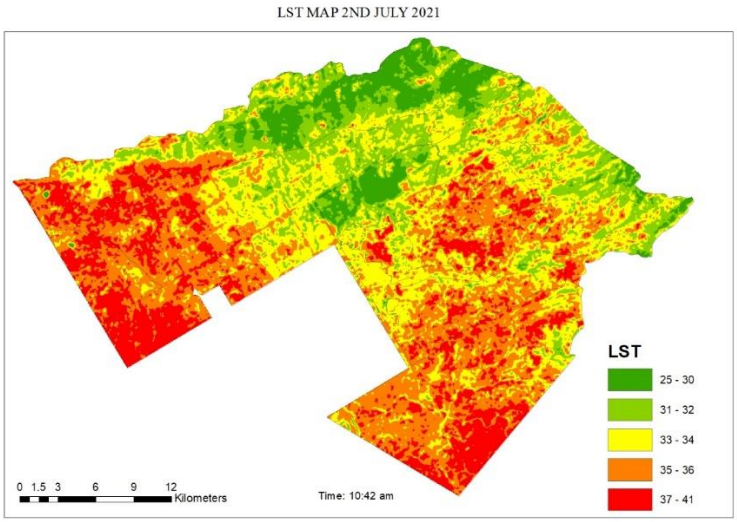

(a)

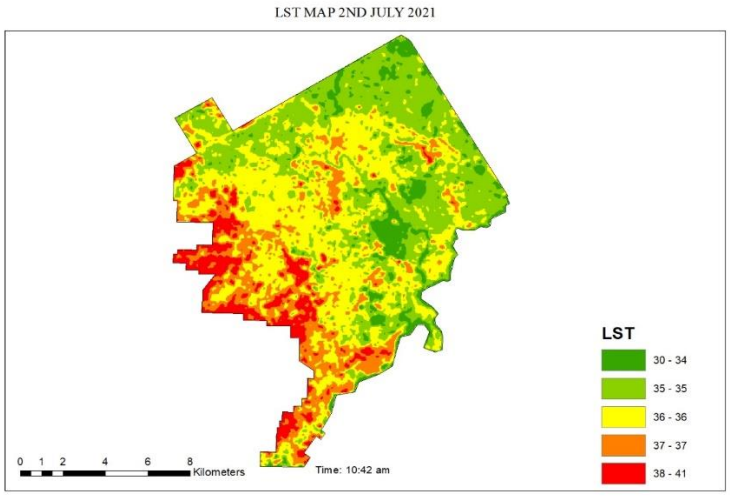

(b)

Model Development and Mesh Generation

The ENVI-met study areas of the twin cities are shown in Figure 3.10. Field survey, as well as the satellite imagery within the Google Earth Pro software, is used to visualize the building footprint, vegetation type, and distribution within each study area of twin cities. AutoCAD was used to delineate building features in the imagery for the generation of 3D models.

Figure 11: Study area maps showing : (a) Twin Cities; (b) ENVI-met study-areas of Islamabad; (c) ENVI-met study-areas of Rawalpindi

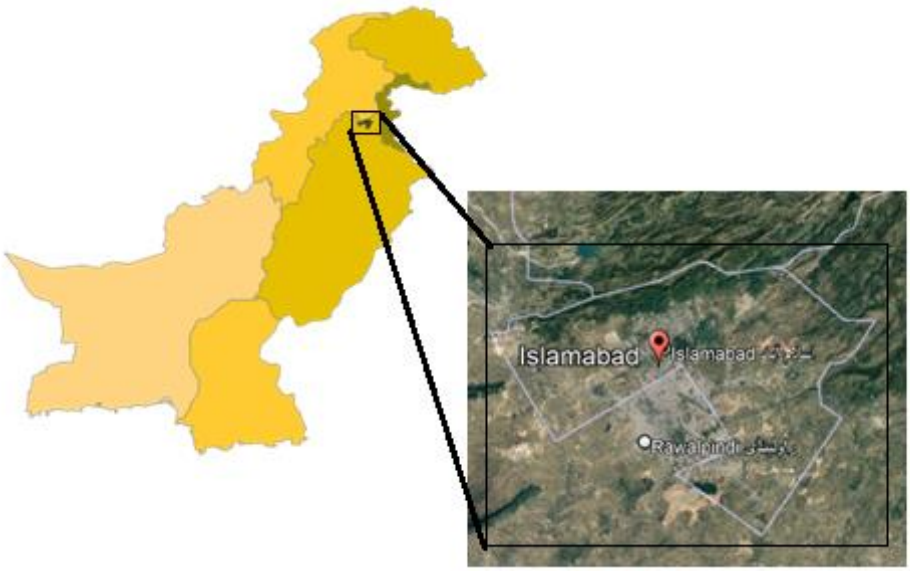

(a)

(b)

(c)

As per CFD best practice guidelines, the computational domain around each study area extends upto10h in both the lateral direction and vertical direction (h is the height of the tallest building). ENVI-met can simulate microclimate with spatial resolutions of 0.5-10m and a temporal resolution of 10 seconds depending on the complexity of the problem and availability of computational resources. In the present study, a constant grid resolution of 2.5m in horizontal and 1m vertical direction is considered as a good compromise between resolution and computation time.

Figure 12: ENVI-Met 3D models of different study sites in Islamabad (A1, A2, A3, and A4), and Rawalpindi (B1, B2, and B3)

A1

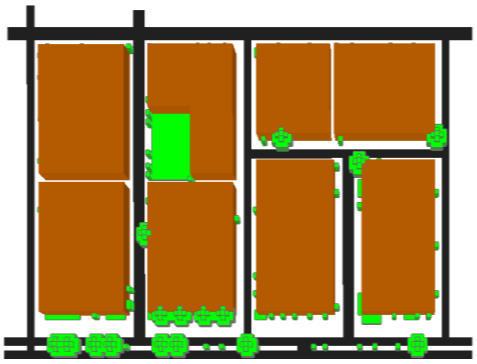

A2

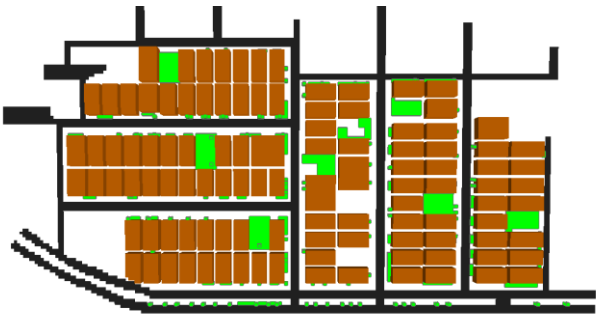

A3

B1

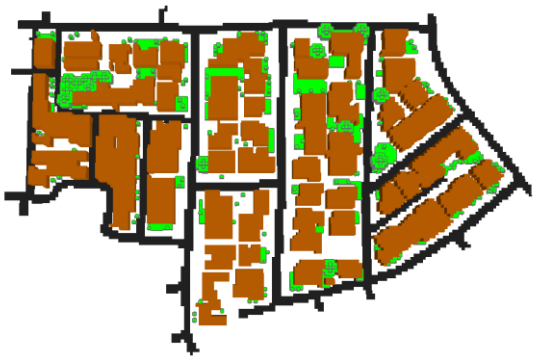

B2

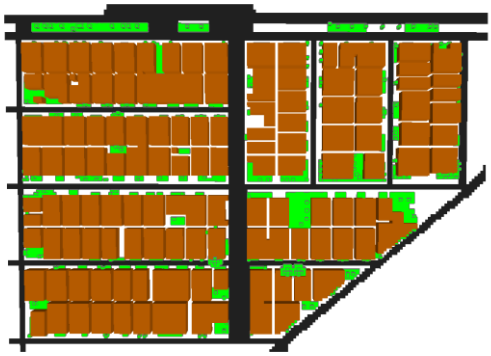

B3

Initial and Boundary Conditions

The simulations are performed for 10th June 2021, the hottest day of summer with the highest temperature of 43° c in the afternoon. The meteorological conditions to force ENVI-met simulations are site-specific hourly air temperature, relative humidity wind speed, and direction data. Full forcing files are attached as Annex A. The forcing of the metrological variable has been proved to be the best measure to increase the accuracy of the results[55].

Building, Soil, and Pavement Material Properties

Building, soil, and pavement properties used as ENVI-met input data are summarized in Table 3.1.

Table 3: ENVI-met Input data

Material Type	Properties
Building Material (Wall & Roof)	The thickness of layers =0.12 and roughness length=0.02m
Soil	Emissivity for longwave thermal radiation=0.98 and roughness length=0.015m
Pavement	Emissivity for longwave thermal radition= 0.9 and reflectivity for shortwave thermal radiation= 0.2 and roughness length=0.01m

In all cases, 14 hours (04:00am to 06:00 pm local standard time) simulations have been performed on a desktop computer with an Intel Core i7-3770K CPU with 16 GB of RAM.

RESULTS AND DISCUSSION

4.1 Effect of Urban Design Elements on Microclimate

As mentioned earlier, the effect of the different urban design elements i.e., street canyon geometry (Canyon length, width, height, orientation, and SVF) and greenery is evaluated the microclimate, thermal comfort, and energy consumption. The three important microclimate indicators considered in the present study are

1. LST
2. Global radiation flux
3. Air temperature

Relationship between the LST and urban design variables

To evaluate the relationship between the LST and different street canyon geometry variables (Canyon length, width, height, orientation, and SVF), around 80different street canyons of Islamabad and Rawalpindi have been selected. The LST values inside this street canyon are extracted from the LST map of twin cities.

The following regression models have been fitted between the dependent and independent variables using the response surface-based method.

LST (Islamabad) = 34.97 + 0.004 **Canyon Orientation** + 2.4011 **SVF** + 0.0568 **Canyon Width** - 0.0486 **Canyon Height**-0.0028**Canyon Length**-0.3190**SVF*Canyon Width**

LST (Rawalpindi)= 35.24-0.0013 **Canyon Orientation** + 0.8863 **SVF**-0.0451**Canyon Width** - 0.0524**Canyon Height**-0.0086**Canyon Length**-0.0065 **SVF*Canyon Orientation** 0.0001**Canyon Orientation*Canyon Length**

For the above relationships, the values of R^2 (47.6% for Islamabad and 77.6% % for Rawalpindi) represent the proportion of variation in LST that can be explained by these regression models.

To check the statistical significance of the individual estimated coefficients, the t-test has been performed (results shown in Tables 4.1 and 4.3). It can be observed that the most of estimated coefficients are statistically significant at 5% levels of significance. The simultaneous significance of the estimated regression coefficients is checked through analysis of variance and the results are presented in Tables 4.2 and 4.4 respectively. The corresponding p-value of the F-statistic shows that both models are adequate at a 5 % level of significance.

Table 4: Coefficients of the estimated regression model for Islamabad with standard errors and t-values

Coefficients	Estimates	SE (Coefficient)	t- value	p-value
Constant	34.3698	0.23495	146.283	0
Greenery Index	-6.0736	2.65306	-2.289	0.025
SVF	2.4011	0.91689	2.619	0.011
Canyon Width	0.0568	0.04280	1.327	0.188
Canyon Height	-0.0486	0.01134	-4.290	0
Canyon Orientation	0.004	0.00022	1.969	0.052
Canyon Length	-0.0028	0.00073	-3.837	0
SVF*Canyon Width	-0.3190	0.15308	-2.084	0.040

R-Sq = 47.61% R-Sq(pred) 38.64%, R Sq(adj)= 42.97%
Note: SE (coefficients) is the standard error of coefficients

Table 5: Analysis of Variance

Source	Degree of freedom	Sum of square	Mean Square	F-ratio	P-value
Regression	7	2.83829	0.405469	10.26	0.000
Error	79	3.12304	0.039532		
Total	86	5.96133			

Table 6: Coefficients of the estimated regression model for Rawalpindi with standard errors and t-values

Coefficients	Estimates	SE (Coefficient)	t- value	p-value
Constant	35.2459	0.11552	305.105	0
SVF	0.8863	0.329136	2.693	0.009
Canyon Width	-0.0451	0.013263	-3.404	0.001
Canyon Height	-0.0524	0.008555	-6.12	0
Canyon Orientation	-0.0013	0.000541	-2.344	0.022
Canyon Length	-0.0086	0.000979	-8.81	0
SVF*Canyon Orientation	-0.0065	0.003113	-2.083	0.041
Canyon Orientation*Canyon Length	0.0001	0.00001	5.375	0

R-Sq = 77.63% R-Sq(pred) 72.69%, R Sq(adj)= 75.29%
Note: SE (coefficients) is the standard error of coefficients

Table 7: Analysis of Variance

Source	Degree of freedom	Sum of square	Mean Square	F-ratio	P-value
Regression	7	4.46664	0.63809	33.21	0.000
Error	67	1.28723	0.01921		
Total	74	5.75387			

It has been observed that in the case of both Islamabad and Rawalpindi, Canyon height has a significant inverse correlation with LST. This is because increasing the canyon height provides shade and prevents the solar radiation from reaching the ground[56–58]. Similarly, canyon width has a positive correlation with LST at 5% levels of significance for both Islamabad and Rawalpindi. Increasing the canyon width amplifies the absorption of the solar radiation thus influencing the LST.

Effect of Urban Design Variables on Global Radiation Fluxes

The hourly mean global radiation at the four different streets having the same orientation but different H/W ratios are presented in Figures 4.1 (a)and (b). It can be observed from these figures that the intensity of global radiation decreases with an increase in H/W ratios. A similar trend in the short-wave radiation fluxes behavior has also been observed by other researchers[27].

Figure 13: Shortwave radiation fluxes received at 1.5 m above the ground for (a) ENE-WSW oriented streets in Islamabad(b) N–S oriented streets in Rawalpindi

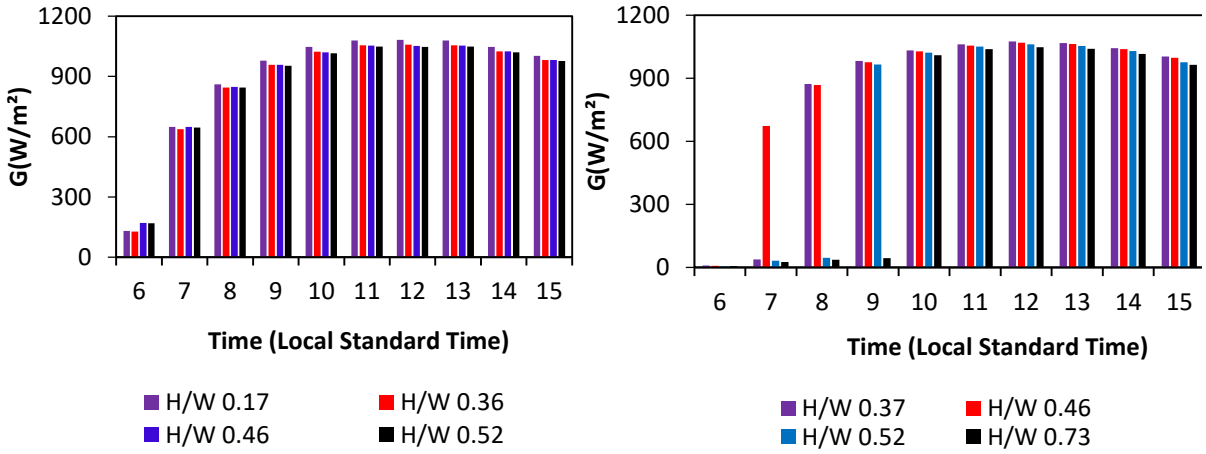

Effect of Urban Design Variables on Air Temperature

Hourly evolution of the air temperature in urban streets having different H/W ratios is shown in Figures4.2 (a) and (b). An inverse relation between the air temperature and the H/W ratio can be observed from both figures. This is because the number of radiations reaching the street space decreases with the increase in the H/W ratio, which results in a decrease in air temperature. A

reduction of 2.1^0 C and 4^0 C in the peak air temperature can be observed due to the increase in the H/W ratio, in the case of Islamabad and Rawalpindi, respectively.

Figure 14: Hourly evolution of the air temperature for (a) ENE-WSW oriented streets in Islamabad(b) N–S oriented streets in Rawalpindi

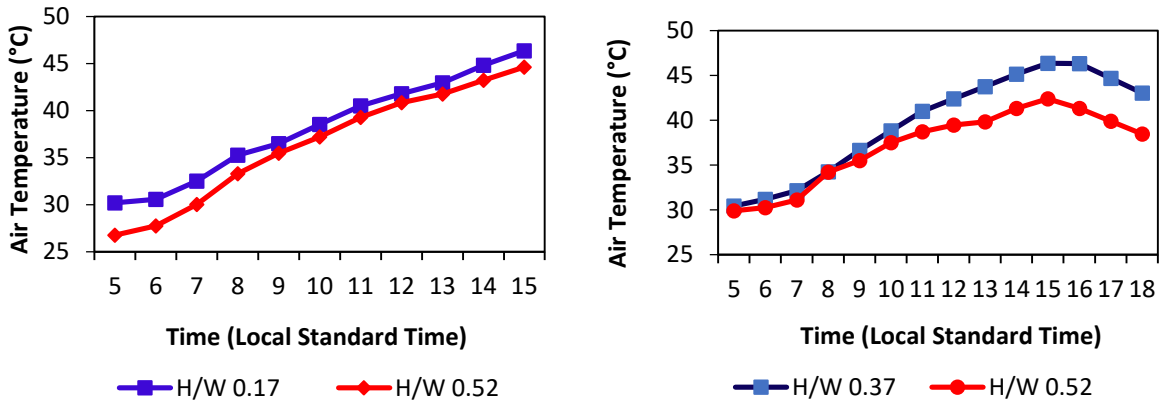

Figures 4.3 (a) and (b) and (c) demonstrate the air temperature variation trend inside the street's canyon having fixed H/W ratios and different orientations (NE-SW and NW-SE in case of Islamabad and E-W, N-S and NE-SW in case of Rawalpindi). It can be observed from Figure 4.3 (a) that street canyons oriented in the NE-SW direction are slightly warmer than NW-SE oriented canyons. Similarly, irrespective of the H/W ratio, the street canyons oriented in the E-W direction are warmer canyon oriented in other directions (N-S and NE-SW) as shown in Figure 4.3 (b) and (c). This is because the warming of the air in a canyon is related to the solar exposure of canyon surfaces. The prolonged solar exposure of E-W and NE-SW-oriented street canyons is the main reason for high heat stress inside these streets[27].

Figure 15: Variation in simulated air temperature for (a) NE-SW and NW-SE, oriented street canyon having H/W=0.46 and 0.52 in Islamabad(b)and (c) E-W, N-S and NE-SW oriented street canyon having H/W=0.73 and 1.22 in Rawalpindi

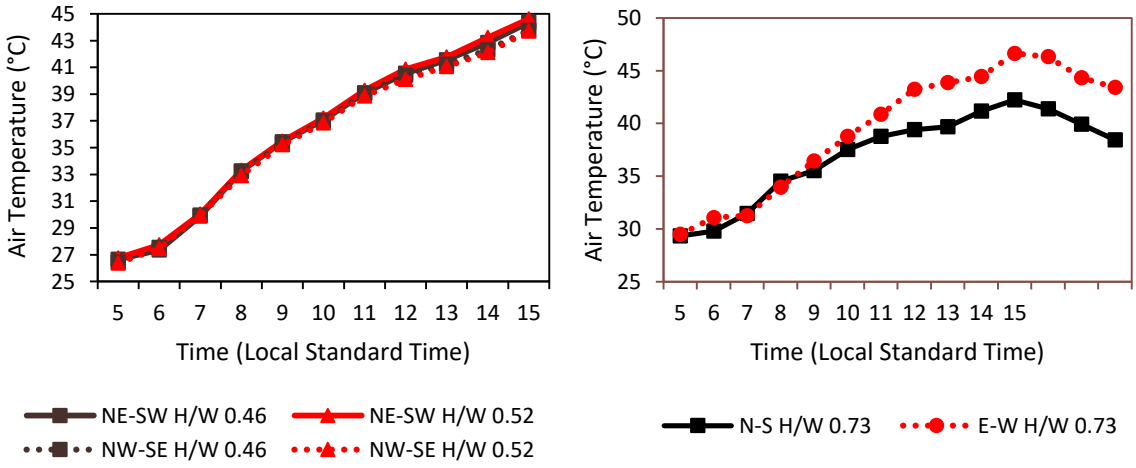

(a) (b)

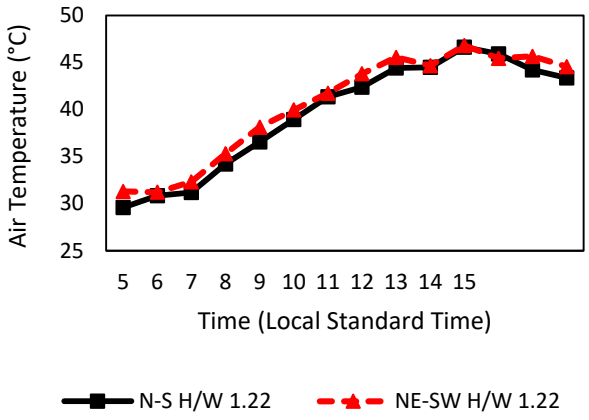

(c)

4.2 Effect of Urban Design Variables on Thermal Comfort

For the current research, the effect of urban design variables is evaluated on two thermal comfort indices i.e., Mean Radiant Temperature (T_{mrt}) and Physiologically Equivalent Temperature (PET). Mean radiant temperature (MRT) is a measure of the average temperature of the surfaces surrounding a particular body, with which it will exchange thermal radiation. It measures the linkages between the outdoor environment and human well-being. ENVI-met calculates T_{mrt} using the following relation[59]

$$T_{mrt} = \left[\frac{1}{\sigma}\left(E_t(z) + \frac{\alpha_k}{\varepsilon_p}\left(D_t(z) + I_t(z)\right)\right)\right]^{0.25}$$

σ is Stefan-Boltzmann constant, $E_t(z)$represents total longwave radiation from ground, walls, and atmosphere, α_k is the absorption coefficient for short wave radiation of the irradiated body surface, ε_p is the human body emissivity, $D_t(z)$ is diffusely reflected solar radiation, and $I_t(z)$ is direct irradiance.

PET is considered to be one of the most popular thermal indexes and is widely used for the assessment of human outdoor thermal comfort. PET is based on the "Munich Energy Balance Model for Individuals" and considers all the relevant environmental factors (i.e. solar radiation, air temperature, humidity, and wind) while keeping thermo-physiological actors (e.g., age, clothing, activity, etc.) to be constant.[60]

Effect of Urban Design Variables on T_{mrt}

Figures 4.4 (a) and (b) present the relationship between T_{mrt} and different H/W ratios per hour of the day. It can be observed that for both Islamabad and Rawalpindi, T_{mrt} has relatively low values in the deep street canyons. This is in agreement with Q. Dai et. al[61] who demonstrated that T_{mrt} decreases with increasing H/W ratios. By increasing the H/W ratios, the reduction in daytime peak T_{mrt} observed for Islamabad and Rawalpindi is 2.28°C and 6.02°C, respectively.

Figure 16: Trend of Tmrt against increasing H/W for (a) ENE-WSW oriented streets in Islamabad, (b) N–S oriented streets in Rawalpindi

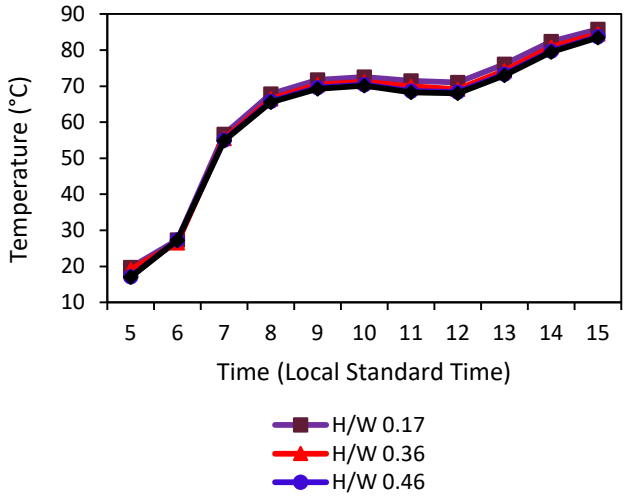

(a)

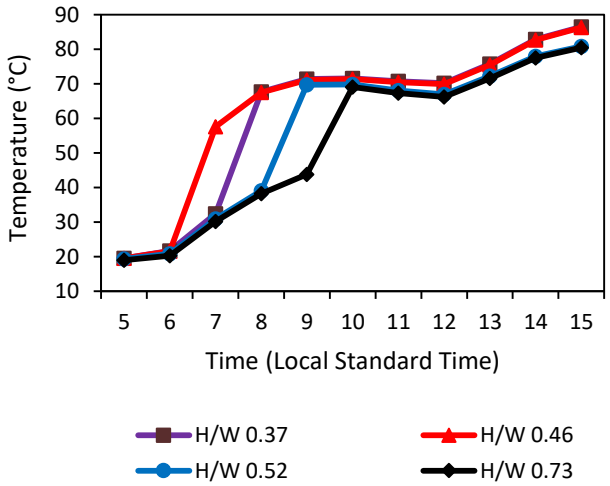

(b)

Effect of Urban Design Variables on PET

Figures 4.5 (a) and (b) depict the hourly evolution of PET in the street having different H/W ratios. Although PET >41^0 (corresponding to an extreme heat stress level) most of the time, a significant increase in the PET peak values with the decrease in H/W ratios can be observed. In the case of Islamabad and Rawalpindi, there is a reduction of 2.3^{0}C and 4.6^{0}C respectively in PET peak values. These results are consistent with findings from previous relevant studies[62].

Figure 17: Variations in daytime PET for (a) ENE-WSW oriented street canyons in Islamabad(b) N–S oriented street canyons in Rawalpindi

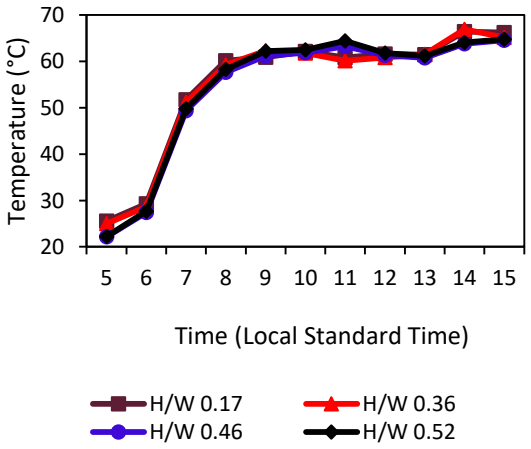

(a)

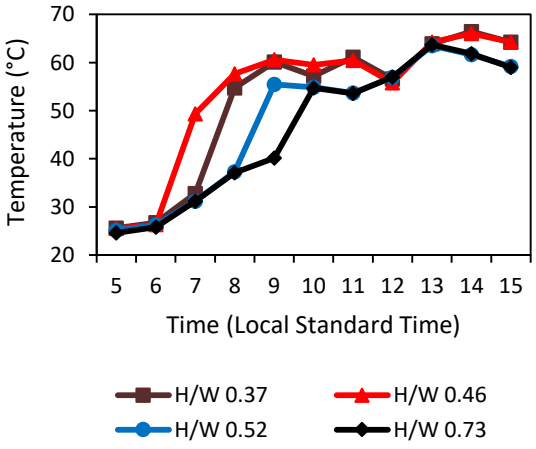

(b)

Figures 4.6 (a), (b), and (c) represent PET differences inside the street canyons having fixed H/W ratios and different orientations (NE-SW and NW-SE in case of Islamabad and E-W, N-S and NE-SW in case of Rawalpindi). It is evident from these figures that regardless of H/W ratios, E-W and NE-SW-oriented streets experience more heat stress and for a longer time than N-S and NW-SE-oriented streets. In the case of Islamabad, NE-SW streets at both H/W ratios are up to 7.5 °C (on PET scale) warmer than NW-SE streets during peak PET times. Similarly, in the case of Rawalpindi, E-W streets having H/W= 0.73 are up to 5.15 °C (on PET scale) warmer than N-S streets during peak PET times.

Figure 18: PET differences inside the streets canyon (a) NE-SW and NW-SE, oriented street canyon having H/W=0.46 and 0.52 in Islamabad (b)and (c) E-W, N-S and NE-SW oriented street canyon having H/W=0.73 and 1.22 in Rawalpindi

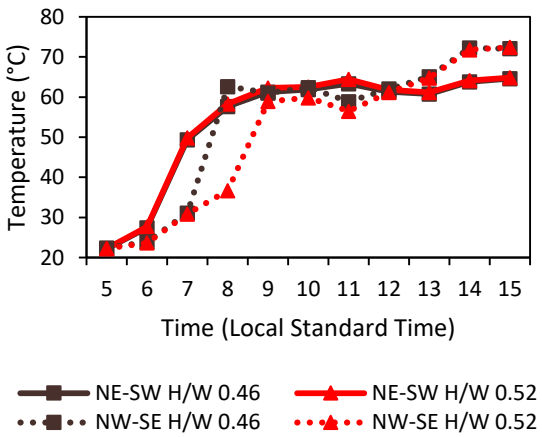

(a)

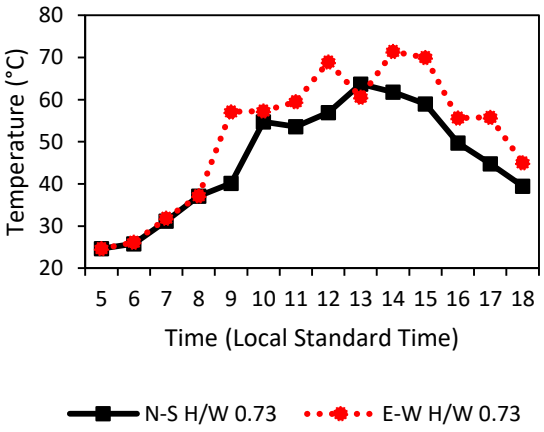

(b)

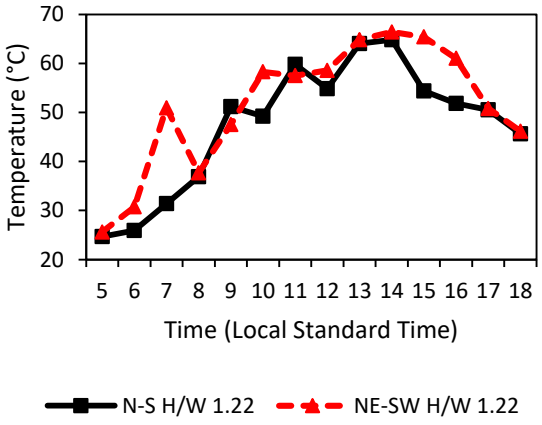

(c)

Figure 4.7 (a), (b), (c) and (d) visualizes the spatial distribution of PET within a street canyon at 1.5m height for NW-SE oriented streets (a and b) and NE-SW oriented streets (c and d). From Figure 4.7 (b) and (c), extreme thermal stress (≥ 41°C PET) can be observed that can observed within the NE-SW oriented street canyon at both H/W ratios. However, a significant reduction in the PET intensity can be observed in the vicinity of trees. Thus, the thermal performance of NE-SW oriented street canyon can be improved by increasing the tree coverage of these streets.

Figure 19: Spatial distribution of PET within a street canyon at 1.5m height for (a) and (b) NW-SE oriented streets (H/W= 0.46, 0.52); (c) and (d) NE-SW oriented streets (H/W= 0.46, 0.52)

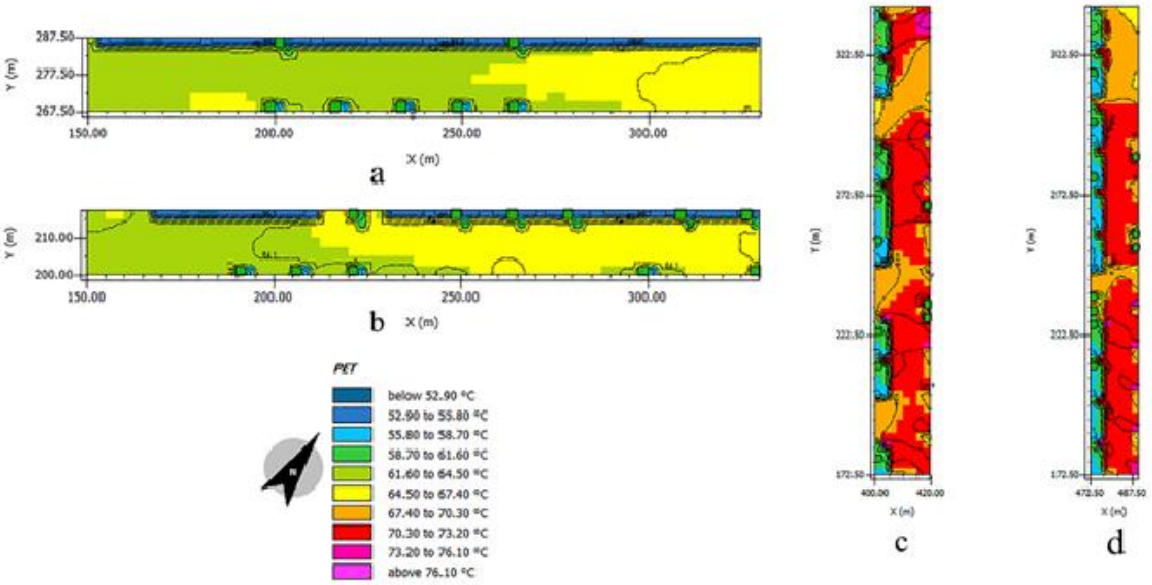

CONCLUSIONS

Our study investigates the effects of urban design elements i.e. street canyon geometry (Canyon length, width, height, orientation, and SVF) and greenery on the urban microclimate using remote sensing and computational fluid dynamics-based techniques. The important conclusion derived from the current research can be used by designers for climate-responsive urban design in case of the future extension of these cities. The important results of the current research are

1. LCZ based LULC classification of the twin cities revealed that the residential area of Islamabad mostly consists of open low-rise buildings. Whereas Rawalpindi residential area is dominated by compact low-rise infrastructure.
2. Being highly urbanized regions, most of the urban areas in twin cities are associated with high LST.
3. According to the regression analysis result, canyon height, width, length have a significant inverse correlation with LST for both cities. This implies that increasing the values of these parameters will bring a prominent cooling effect. The skyview factor is has a significant positive correlation with LST in both cities. So by decreasing skyview factors either by (i) introducing the deep street canyons or (i) increasing the greenery inside the wide canyon will reduce the LST intensity inside these street canyons
4. According to the CFD simulation results,
    a. The intensity of global radiation decreases with an increase in H/W ratios
    b. An inverse relation between the air temperature and the H/W ratio can be observed for both cities. A reduction of 2.1^0 C and 4^0 C in the peak air temperature has been observed due to the increase in H/W ratios in the case of Islamabad and Rawalpindi, respectively.
    c. In case of Islamabad, street canyons oriented in the NE-SW direction are slightly warmer than NW-SE oriented canyons. Similarly in the case of Rawalpindi, irrespective of the H/W ratio, the street canyons oriented in the E-W direction are warmer than canyons oriented in other directions (N-S and NE-SW)
    d. For both cities i.e. Islamabad and Rawalpindi, T_{mrt} has relatively low values in the deep street canyons.
    e. In the case of Islamabad and Rawalpindi, a reduction of 2.3^0C and 4.6^0C respectively in PET peak values has been noticed due to the increase in H/W ratios.
    f. In the case of Islamabad, NE-SW streets are up to 7.5 °C (on PET scale) warmer than NW-SE streets during peak PET times. Similarly, in the case of Rawalpindi, E-W streets having H/W= 0.73 are up to 5.15 °C (on PET scale) warmer than N-S streets during peak PET times.
    g. However, a significant reduction in the PET intensity has been observed in the vicinity of trees. Thus, the thermal performance of a street canyon can be improved by increasing the tree coverage of these streets

5.1 Policy Recommendations

1. The instant study underscores the significance of altering the contemporary regulations and bylaws to encourage more efficient layouts and elevations - such as vertical construction.
2. The magnitude of the impact of different urban design variables on urban microclimate, and outdoor comfort may vary from city to city, an appropriate scientific intervention ought to be followed at the very inception stage to ensure a climate-responsive urban planning and design.

REFERENCES

Elmqvist, T., Redman, C. L., Barthel, S., & Costanza, R. (2013). History of urbanization and the missing ecology. In *Urbanization, biodiversity and ecosystem services: Challenges and opportunities* (pp. 13–30). Springer, Dordrecht.

Zhang, X. Q. (2016). The trends, promises and challenges of urbanisation in the world. *Habitat International*, *54*, 241–252.

Masson-Delmotte, V., Zhai, P., Pörtner, H.-O., Roberts, D., Skea, J., Shukla, P. R., Pirani, A., Moufouma-Okia, W., Péan, C., Pidcock, R., & others. (2018). Global warming of 1.5 C. *An IPCC Special Report on the Impacts of Global Warming Of*, *1*(5).

Ribeiro, H. V, Rybski, D., & Kropp, J. P. (2019). Effects of changing population or density on urban carbon dioxide emissions. *Nature Communications*, *10*(1), 1–9.

Esch, T., Heldens, W., Hirner, A., Keil, M., Marconcini, M., Roth, A., Zeidler, J., Dech, S., & Strano, E. (2017). Breaking new ground in mapping human settlements from space--The Global Urban Footprint. *ISPRS Journal of Photogrammetry and Remote Sensing*, *134*, 30–42.

Edenhofer, O. (2015). *Climate change 2014: mitigation of climate change* (Vol. 3). Cambridge University Press.

Johansson, T. B., Patwardhan, A. P., Nakićenović, N., & Gomez-Echeverri, L. (2012). *Global energy assessment: toward a sustainable future*. Cambridge University Press.

Bai, X., McPhearson, T., Cleugh, H., Nagendra, H., Tong, X., Zhu, T., & Zhu, Y.-G. (2017). Linking urbanization and the environment: Conceptual and empirical advances. *Annual Review of Environment and Resources*, *42*, 215–240.

Chaudhry, Q. U. Z. (2017). *Climate change profile of Pakistan*. Asian development bank.

Kershaw, T. (2017). *Climate Change Resilience in the Urban Environment*. IOP Publishing.

Metternicht, G. (2017). Land use planning. *Global Land Outlook (Working Paper)*.

Chen, Y.-J., Matsuoka, R. H., & Liang, T.-M. (2018). Urban form, building characteristics, and residential electricity consumption: A case study in Tainan City. *Environment and Planning B: Urban Analytics and City Science*, *45*(5), 933–952.

Yang, J., Shi, B., Xia, G., Xue, Q., & Cao, S.-J. (2020). Impacts of urban form on thermal environment near the surface region at pedestrian height: A case study based on high-density built-up areas of Nanjing City in China. *Sustainability*, *12*(5), 1737.

Emmanuel, R., & Steemers, K. (2018). Connecting the realms of urban form, density and microclimate. In *Building Research & Information* (Vol. 46, Issue 8, pp. 804–808). Taylor & Francis.

Martilli, A. (2007). Current research and future challenges in urban mesoscale modelling. *International Journal of Climatology: A Journal of the Royal Meteorological Society*, *27*(14), 1909–1918.

Varentsov, M. I., Grishchenko, M. Y., & Wouters, H. (2019). Simultaneous assessment of the

summer urban heat island in Moscow megacity based on in situ observations, thermal satellite images and mesoscale modeling. *Geography, Environment, Sustainability*, *12*(4), 74–95.

Gedzelman, S. D., Austin, S., Cermak, R., Stefano, N., Partridge, S., Quesenberry, S., & Robinson, D. A. (2003). Mesoscale aspects of the urban heat island around New York City. *Theoretical and Applied Climatology*, *75*(1), 29–42.

Göndöcs, J., Breuer, H., Pongrácz, R., & Bartholy, J. (2017). Urban heat island mesoscale modelling study for the Budapest agglomeration area using the WRF model. *Urban Climate*, *21*, 66–86.

Sokhi, R. S., Baklanov, A., & Schlünzen, K. H. (2018). *Mesoscale Modelling for Meteorological and Air Pollution Applications*. Anthem Press.

Baik, J.-J., Park, S.-B., & Kim, J.-J. (2009). Urban flow and dispersion simulation using a CFD model coupled to a mesoscale model. *Journal of Applied Meteorology and Climatology*, *48*(8), 1667–1681.

Bherwani, H., Singh, A., & Kumar, R. (2020). Assessment methods of urban microclimate and its parameters: A critical review to take the research from lab to land. *Urban Climate*, *34*, 100690.

Toparlar, Y., Blocken, B., Maiheu, B., & Van Heijst, G. J. F. (2017). A review on the CFD analysis of urban microclimate. *Renewable and Sustainable Energy Reviews*, *80*, 1613–1640.

Howard, L. (1820). *The Climate of London: Deduced from Meteorological Observations Made at Different Places in the Neighbourhood of the Metropolis. In Two Volumes. Vol. II.* (Vol. 2). W. Phillips.

Mirzaei, P. A., & Haghighat, F. (2010). Approaches to study urban heat island--abilities and limitations. *Building and Environment*, *45*(10), 2192–2201.

Mirzaei, P. A. (2015). Recent challenges in modeling of urban heat island. *Sustainable Cities and Society*, *19*, 200–206.

Rajkovich, N. B., & Larsen, L. (2016). A bicycle-based field measurement system for the study of thermal exposure in Cuyahoga County, Ohio, USA. *International Journal of Environmental Research and Public Health*, *13*(2), 159.

Ali-Toudert, F., & Mayer, H. (2006). Numerical study on the effects of aspect ratio and orientation of an urban street canyon on outdoor thermal comfort in hot and dry climate. *Building and Environment*, *41*(2), 94–108.

Arnfield, A. J. (2003). Two decades of urban climate research: a review of turbulence, exchanges of energy and water, and the urban heat island. *International Journal of Climatology: A Journal of the Royal Meteorological Society*, *23*(1), 1–26.

Abreu-Harbich, L. V, Labaki, L. C., & Matzarakis, A. (2014). Thermal bioclimate in idealized urban street canyons in Campinas, Brazil. *Theoretical and Applied Climatology*, *115*(1), 333–340.

Jareemit, D., & Srivanit, M. (2019). Effect of Street Canyon Configurations and Orientations on Urban Wind Velocity in Bangkok Suburb Areas. *IOP Conference Series: Materials Science and Engineering*, *690*(1), 12006.

Ali-Toudert, F., & Mayer, H. (2007). Effects of asymmetry, galleries, overhanging facades and vegetation on thermal comfort in urban street canyons. *Solar Energy*, *81*(6), 742–754.

Achour-Younsi, S., & Kharrat, F. (2016). Outdoor thermal comfort: impact of the geometry of an urban street canyon in a Mediterranean subtropical climate–case study Tunis, Tunisia. *Procedia-Social and Behavioral Sciences*, *216*, 689–700.

Ketterer, C., & Matzarakis, A. (2014). Human-biometeorological assessment of heat stress reduction by replanning measures in Stuttgart, Germany. *Landscape and Urban Planning*, *122*, 78–88.

Sharmin, T., Steemers, K., & Matzarakis, A. (2017). Microclimatic modelling in assessing the impact of urban geometry on urban thermal environment. *Sustainable Cities and Society*, *34*, 293–308.

Taleghani, M., Kleerekoper, L., Tenpierik, M., & Van Den Dobbelsteen, A. (2015). Outdoor thermal comfort within five different urban forms in the Netherlands. *Building and Environment*, *83*, 65–78.

Delpak, N., Sajadzadeh, H., Hasanpourfard, S., & Aram, F. (2021). *The Effect of Street Orientation on Outdoor Thermal Comfort in a Cold Mountainous Climate*.

Alznafer, B. M. (2014). *The impact of neighbourhood geometries on outdoor thermal comfort and energy consumption from urban dwellings: a case study of the Riyadh city, the kingdom of Saudi Arabia*. Cardiff University.

Yin, S., Lang, W., & Xiao, Y. (2019). The synergistic effect of street canyons and neighbourhood layout design on pedestrian-level thermal comfort in hot-humid area of China. *Sustainable Cities and Society*, *49*, 101571.

Habitat, U. N. (2020). World Cities Report 2020: The value of sustainable urbanization. In *Nairobi, Kenya*.

Boeing, G. (2017). OSMnx: New methods for acquiring, constructing, analyzing, and visualizing complex street networks. *Computers, Environment and Urban Systems*, *65*, 126–139.

Peel, M. C., Finlayson, B. L., & McMahon, T. A. (2007). Updated world map of the Köppen-Geiger climate classification. *Hydrology and Earth System Sciences*, *11*(5), 1633–1644.

Ziaul, S. K., & Pal, S. (2016). Image based surface temperature extraction and trend detection in an urban area of West Bengal, India. *Journal of Environmental Geography*, *9*(3–4), 13–25.

McMillin, L. M. (1975). Estimation of sea surface temperatures from two infrared window measurements with different absorption. *Journal of Geophysical Research*, *80*(36), 5113–5117.

Soleimani Vosta Kolaei, F., & Akhoondzadeh, M. (2018). A comparison of four methods for extracting Land Surface Emissivity and Temperature in the Thermal Infrared Hyperspectral Data. *Earth Observation and Geomatics Engineering*, *2*(1), 56–63.

Sobrino, J. A., Jiménez-Muñoz, J. C., & Paolini, L. (2004). Land surface temperature retrieval from LANDSAT TM 5. *Remote Sensing of Environment*, *90*(4), 434–440.

Kant, Y., & Badarinath, K. V. S. (1998). A method for estimating the land surface temperature from

satellite data using emissivity derived from vegetation index. *Current Science*, 139–145.

Tan, K. C., Lim, H. S., MatJafri, M. Z., & Abdullah, K. (2010). Landsat data to evaluate urban expansion and determine land use/land cover changes in Penang Island, Malaysia. *Environmental Earth Sciences*, *60*(7), 1509–1521.

Sobrino, J. A., Raissouni, N., & Li, Z.-L. (2001). A comparative study of land surface emissivity retrieval from NOAA data. *Remote Sensing of Environment*, *75*(2), 256–266.

Rouse, J. W., Haas, R. H., Schell, J. A., & Deering, D. W. (1974). Monitoring vegetation systems in the Great Plains with ERTS: Proceedings of the Third Earth Resources Technology Satellite-1 Symposium. *NASA SP-351*, 301–317.

Tominaga, Y., Mochida, A., Yoshie, R., Kataoka, H., Nozu, T., Yoshikawa, M., & Shirasawa, T. (2008). AIJ guidelines for practical applications of CFD to pedestrian wind environment around buildings. *Journal of Wind Engineering and Industrial Aerodynamics*, *96*(10–11), 1749–1761.

Blocken, B. (2015). Computational Fluid Dynamics for urban physics: Importance, scales, possibilities, limitations and ten tips and tricks towards accurate and reliable simulations. *Building and Environment*, *91*, 219–245.

Franke, J., Hellsten, A., Schlünzen, K. H., & Carissimo, B. (2007). Best practice guideline for the CFD simulation of flows in the urban environment-a summary. *11th Conference on Harmonisation within Atmospheric Dispersion Modelling for Regulatory Purposes, Cambridge, UK, July 2007*.

Stavrakakis, G. M., Katsaprakakis, D. Al, & Damasiotis, M. (2021). Basic Principles, Most Common Computational Tools, and Capabilities for Building Energy and Urban Microclimate Simulations. *Energies*, *14*(20), 6707.

Tsoka, S., Tsikaloudaki, K., Theodosiou, T., & Bikas, D. (2020). Urban Warming and Cities' Microclimates: Investigation Methods and Mitigation Strategies—A Review. *Energies*, *13*(6), 1414.

Salvati, A., & Kolokotroni, M. (2019). Microclimate data for building energy modelling: Study on ENVI-met forcing data. *16th IBPSA Conference Rome, Italy, Sept. 2-4, 2019*, 3361–3368.

Wang, M., & Xu, H. (2021). The impact of building height on urban thermal environment in summer: A case study of Chinese megacities. *Plos One*, *16*(4), e0247786.

Yu, K., Chen, Y., Wang, D., Chen, Z., Gong, A., & Li, J. (2019). Study of the seasonal effect of building shadows on urban land surface temperatures based on remote sensing data. *Remote Sensing*, *11*(5), 497.

Watanabe, S., Nagano, K., Ishii, J., & Horikoshi, T. (2014). Evaluation of outdoor thermal comfort in sunlight, building shade, and pergola shade during summer in a humid subtropical region. *Building and Environment*, *82*, 556–565.

Yang, F., Lau, S. S. Y., & Qian, F. (2011). Thermal comfort effects of urban design strategies in high-rise urban environments in a sub-tropical climate. *Architectural Science Review*, *54*(4), 285–304.

Höppe, P. (1999). The physiological equivalent temperature--a universal index for the biometeorological assessment of the thermal environment. *International Journal of*

Biometeorology, *43*(2), 71–75.

Dai, Q., Schnabel, M. A., & Heusinkveld, B. (2012). Influence of height-to-width ratio: Case study on mean radiant temperature for Netherlands buildings. *Proceedings of the 46th Annual Conference of the Architectural Science Association (ASA 2012), Queensland, Australia*, 14–16.

Lobaccaro, G., Acero, J. A., Sanchez Martinez, G., Padro, A., Laburu, T., & Fernandez, G. (2019). Effects of orientations, aspect ratios, pavement materials and vegetation elements on thermal stress inside typical urban canyons. *International Journal of Environmental Research and Public Health*, *16*(19), 3574.